PROCEEDINGS OF SCIENCE

Expectation on Observation of Cosmic Rays Energy Spectrum from 10PeV to 100PeV with LHAASO Experiment

Lingling Ma*
for LHAASO collaboration
E-mail: llma@ihep.ac.cn

Measurement of individual cosmic ray species in a broad energy range from 50 TeV to sub-EeV is one of main goals of LHAASO experiment. In order to cover the broad energy range, the observations are divided into three stages, which are from 50 TeV to 10 PeV, from 10 PeV to 100 PeV, from 100 PeV to EeV. In this paper, we present a preliminary investigation on the capability of particle identification, energy resolution and effective aperture in the second stage by using one square kilometer detector array LHAASO-KM2A and 18 wide field Cherenkov telescopes in LHAASO-WFCTA.

35th International Cosmic Ray Conference ICRC2017
10-20 July, 2017
Bexco, Busan, Korea

*Speaker.

PoS(ICRC2017)549

1. Introduction

Although the cosmic rays have been discovered for more than 100 years, the questions about their origin and acceleration have not been answered clearly. Galactic cosmic rays are mainly believed to originate at astrophysical sources, such as supernova remnants. Since most cosmic rays are charged particles, they are deflected by irregular galactic magnetic fields, the arrival directions cannot be used to identify their sources. But measurements of their energy spectra are very important to resolve the questions, especially the measurements of energy spectra for individual elements. The energy spectrum of cosmic rays follows a simple power law over a very broad energy range from 10^9 eV to 10^{20} eV[1]. Only a handful of significant features are shown over the whole energy range. One of them is a change in the spectral index at 3×10^{15} eV, generally called the knee[2]. Several theories for the origin of the knee predict different knee positions for particles of different elements. One of the theories is that the knee marks the highest energy that the galactic cosmic ray sources can reach, taking into account the extension of the acceleration region and the strength of the magnetic field. The knee in the energy spectrum of all cosmic rays is mainly caused by the steepening of the energy spectra of the light components[3]. Therefore the energy spectra of single elements or at least mass groups are considered to be interest. The energy spectra for individual elements are obtained directly with space-borne experiments at the top of the atmosphere. But limited by the effective area of the experiments and the rapidly falling flux of cosmic rays, the statistically reliable measurements can only reach up to 100 TeV. Measurements at higher energies require large detection areas or long exposure time, which presently can only be realized in ground-based experiments. These experiments detect the extensive air showers (EAS) produced by the interactions of cosmic particles with nuclei of the Earth's atmosphere. Since the ground-based experiments can only sample the secondary particles in the EAS, the determination of spectra for individual elements or mass group is limited by the large intrinsic fluctuations of EAS. Furthermore, the measurements on the ground rely on the simulation results and the hadronic interaction models. So the energy scales of the ground-based experiments can't be calibrated easily, which affect the positions of the knee. Therefore, different experiments find different knee energies. In addition, the nature of the primary cosmic rays can't be identified directly and effectively. With large uncertainties, the knee positions of different elements can't be determined clearly, and thus constrict the theory of the origin and acceleration of cosmic rays.

Large High Altitude Air Shower Observatory (LHAASO) can improve the situations. With three major detector arrays (LHAASO-WCDA, LHAASO-KM2A, LHAASO-WFCTA), one of the main aims of LHAASO is to measure the energy spectra from $50TeV$ to sub-EeV for individual cosmic ray elements with an absolute energy scale.

In this papaer, the LHAASO detectors are described in sec 2. The simulation of the detectors and analysis are described in sec 3. The performance of the detectors are shown in sec 4 and sec 5.

2. LHAASO detector arrays and observation stages

LHAASO-WCDA is a water Cherenkov detector array with a total area of $78{,}000m^2$. LHAASO-WCDA consists of three water pools with a depth of 4.5m and divided into 900 cells with $5m \times 5m$. One of the pools has has two type PhotoMultiplier Tubes (PMT) anchored on the bottom at the cen-

ter of the cell and the dynamic range can be achieved from 2800 to 28,000,000 PEs. High energy components in the EAS near the core can be measured. The high energy components produced in the last few generations, thus the parameter is sensitive to the identity of the primary particle.

LHAASO-KM2A includes a muon detector array using water Cherenkov technique with 40,000 m^2 and an electromagnetic particle array with 5635 scintillator detectors. The spacing of the scintillator detectors is set to as 15 m, while the spacing of the muon detectors is set to as 30 m. The two arrays can cover $1km^2$. With the largest muon detector array, the number and lateral distribution of muon can be measured and they are sensitive to the identity of the primary particle.

LHAASO-WFCTA is a wide field Cherenkov telescope array with 18 telescopes. Each telescope has a light collecting area of $5m^2$ and a camera of 1024 pixels. Pixel detector is a SiPM followed by a flash A/D convertor-based (FADC) front end electronics (FEE). All components of the telescope are placed in a container. Thus, the telescope array can be easily moved and rearranged. The total number of photoelectrons in the Cherenkov image is a good shower energy estimator. While the shape of the image contains the information of the shower maximum position, thus it is a parameter sensitive to the identify primary particles.

In order to cover a broad energy range, the re-arrangement of LHAASO-WFCTA is necessary. So the observation of the energy spectrum is divided into four stages, which are in charge of from $50TeV$ to $100TeV$, from $100TeV$ to $10PeV$, from $10PeV$ to $100PeV$ and from $100PeV$ to $sub-EeV$. In the first stage, the absolute energy scale have to be obtained by cross calibrating with the space-bone experiments. In the second stage, the knee of proton or the light elements can be measured. In the third stage, the knee of iron or the heavy elements can be measured. In the fourth stage, in order to enlarge the effective area, the WFCTA telescopes have to be changed into fluorescence mode and placed $5km$ away from the center of LHAASO. In this paper, the performance and arrangement of different type detectors in the third stages are studied by detail simulations.

3. Simulations and reconstructions

In the third stage,due to the high energy of air showers, the detectors of LHAASO-WCDA are saturated, so it is not used in the stage. Only LHAASO-KM2A and LHAASO-WFCTA are used in the stage.

The shower maximum positions of cosmic rays in the energy range are from $500g/cm^2$ to $650g/cm^2$. Considering the air depth of LHAASO site $600g/cm^2$, the showers with zenith angle around 45° in the energy range can be fully developed. Thus, the telescopes are pointed to the zenith 45°. In order to achieve hybrid observation with LHAASO-KM2A, the telescopes are placed near center of the array. In addition, in the energy range, the number of Cherenkov photons is very huge, in order to avoid of the saturation of the telescopes, a filter is used at the door of the container to select photons with wavelength range from $300nm$ to $400nm$.

The simulation of LHAASO detectors is divided into two steps. The first step is to simulate air showers initiated by cosmic rays using CORSIKA program[4]. In the CORSIKA program, EGS4 model is chosen for electromagnetic process and QJSJET-II04 and FLUKA models are chosen for high and low energy hadronic process, respectively. In this stage, the absorption and scattering of Cherenkov photons in the atmosphere are considered. In order to save the CPU consumption and the disk memory, on one hand the quantum efficiency of PMTs are considered, on the other hand

the thinning option is selected during the shower generation by CORSIKA. Besides Cherenkov data, the particles data are also recorded to do a hybrid observation.

Five compositions proton, helium, CNO, MgAlSi and iron with energy from 10PeV to 100PeV are generated according to a power law spectrum with a spectral index of -1. For each composition, 5000 events are generated. For each event, it is reused for 20 times. According to the FOV covered by the LHAASO-WFCTA, the directions of the generated showers are from 35° to 55° in zenith and from 0° to 360° in azimuth.

The second step is the detector simulations including LHAASO-WFCTA and LHAASO-KM2A. The simulation of LHAASO-WFCTA contains 3 steps. The first one is the ray tracing model which deals with the process after the Cherenkov photons entering the telescopes. The roughness and the pointing errors of each mirror are simulated in the ray tracing procedure. The second one is the camera simulation which deals with the night sky simulation and electronics simulation. The third one is the trigger simulation.

The simulation of LHAASO-KM2A is done by fast simulation. In the simulation, the detection efficiency of the muon detectors and the electromagnetic detectors to the muons, electron/positrons and gammas are considered. The detection efficiency is obtained by the detail gant4 simulation of single detectors. And it is the function of the energy and the incident angle of the muons, electrons/positrons and gammas.

The geometry reconstruction including the shower core positions and the arriving directions of the shower can be obtained by LHAASO-KM2A with resolution of 3m and 0.3°, respectively.

The shower energy, E, is reconstructed using the total number of Cherenkov photo-electrons, Npe, collected by the telescope. At the energy range, the shoulders of the lateral distributions of the Cherenkov photons for high energy events are disappeared. The number of Cherenkov photons exponentially drops with impact parameter Rp and therefore the effect has to be taken into account in the shower energy determination[5]. So the shower energy is a function of Npe and Rp, and a look-up table for the shower energy with two entries, i.e., Npe and Rp can be obtained. For a shower with Npe measured by the LHAASO-WFCTA and Rp measured by the LHAASO-KM2A, the energy of the shower can be read out from the look-up table.

In order to get a full Cherenkov image, some cuts are used, such as, the arrival directions of the shower should be in a circle with the 4° radius and centered in the center of the FOV of the telescope. In order to avoid the saturation of PMTs, the showers with Rp less than 50m are discarded due to the huge number of Cherenkov photons. In addition, the showers with Rp larger than 300m are also discarded, due to the large fluctuations of the Cherenkov photons. With these cuts, the energy resolution is found symmetric and fits well a Gaussian function with σ about 22% as shown in figure 1.

4. Identification of primary particles

Showers induced by heavy primaries start earlier in the atmosphere and the higher nucleon number leads to a relatively larger muon content at observation level. The fraction of muons of all particles in the shower at observation level is characteristic for the primary mass. LHAASO-KM2A with the greatest muon detectors array and electromagnetic detectors array can measure the muon and electromagnetic particles very well including their total numbers and lateral distributions.

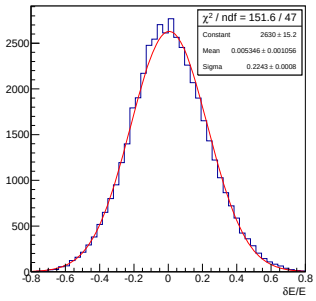

Figure 1: The energy resolution obtained by LHAASO-WFCTA. The red line shows the Gaus fit.

Because the higher the energy of the primary cosmic ray the larger the total particle number, the ratio of total electromagnetic particles and muon P_r measured by LHAASO-KM2A are used to reduce the energy effects. The relation between P_r and the primary energy of showers are shown in figure 2 (left). In order to measure the electromagnetic particles and the muons without bias of geometry, events with core located in a circle with radius from 180m to 500m and centered at the center of the array are chosen. For radius less than 180m, LHAASO-WCDA is located and doesn't have the LHAASO-KM2A detectors. For radius larger than 500m, it is out the range of LHAASO-KM2A.

From figure 2, the energy dependent is still existed. After energy correction the distributions of P_r-3.5$\times log10(Energy)$ is shown in figure 3. The lines shown in the left plot are normalized to 1, while the lines in the right plot are normalized to the expectation of Horandel model.

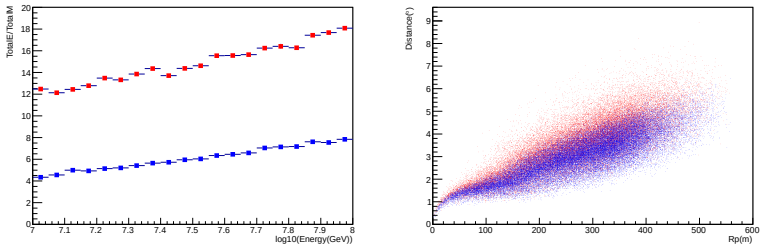

Figure 2: left:The relationship between ratio of total electromagnetic particles and muons measured by LHAASO-KM2A and the primary energy of the showers. right: The relationship between the centroid of the image and the arrival direction of the shower.The red squares indicate the proton, while the blue ones indicate the iron.

The LHAASO-WFCTA watches shower longitudinal development from a distance of Rp and take it as the shower image in the camera. Because the shower geometry is precisely reconstructed by the LHAASO-KM2A, the distribution of number of photoelectrons in the image along the shower axis describes the shower profile at certain precision. The centroid of the image indicates the shower maximum position in sky while the direction of the shower points the start of the shower. So the angular distance $\delta\theta$ between the centroid of the image and the arrival direction of the shower could be used to measure the atmospheric depth for shower maximum. However, the image is stretched longer for farther showers due to pure geometric effect. The stretched effects

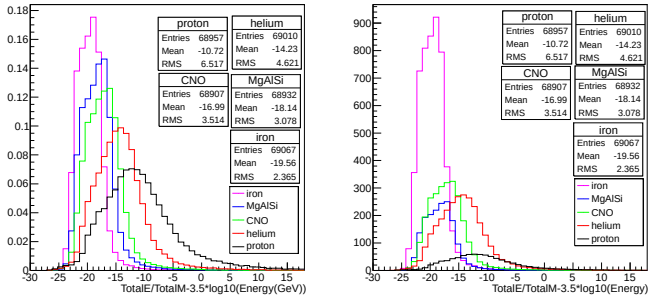

Figure 3: The distributions of P_r after energy corrections. The distributions in the left plot are normalized to 1, while the lines in the right plot are normalized to the expectation of Horandel model

are shown in figure 2 (right). In order to get a full Cherenkov image, the same cuts are used as in the energy reconstruction.

The stretched effects are corrected $\delta\theta - 0.0084 \times Rp$. After correction, the distribution of $\delta\theta - 0.0084 \times Rp$ are shown in figure 4. The lines shown in the left plot are normalized to 1, while the lines in the right plot are normalized to the expectation of Horandel model. About 30% separation between protons and irons can be seen from figure 4.

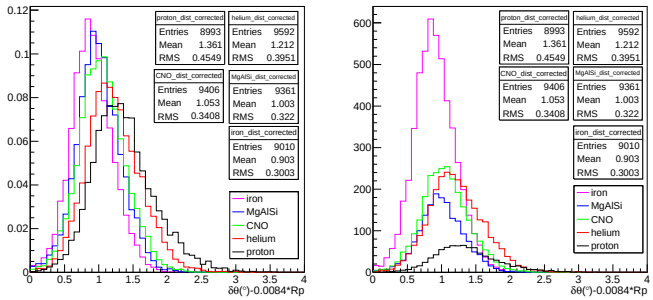

Figure 4: The distributions of $\delta\theta$ after Rp corrections. The distributions in the left plot are normalized to 1, while the lines in the right plot are normalized to the expectation of Horandel model

The correlation between P_r and $\delta\theta$ is also studied in figure 5. If the P_r with values less than -20 and $\delta\theta$ with values less than 0.8 are selected, the contamination of iron is about 13% with 25% selection efficiency of iron, while the contamination of iron and MgAlSi is about 6%.

5. Effective area and event rate

Besides the capability in the discrimination of primary elements, the effective area is another important property of the experiments which are focused on the measurements of cosmic ray spectra. In order to enlarge the effective area, the overlap of FOV of the telescopes of WFCTA is reduced as little as possible by setting different pointing direction in azimuth. The interval in azimuth pointing between two neighbor telescopes is set to be 20°.

The hybrid effective areas of LHAASO-KM2A and LHAASO-WFCTA with 18 telescopes at different energies are studied and are shown in figure 6 (left). In order to get high quality

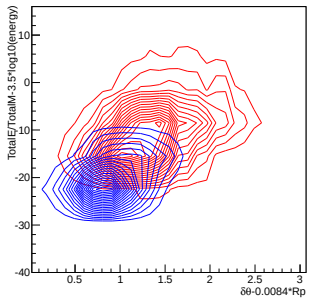

Figure 5: The correlation between P_r obtained by LHAASO-KM2A and $\delta\theta$ obtained by LHAASO-WFCTA. The red lines indicate the proton, while the blue lines indicate the iron.

events some cuts are chosen in the figure 6 (left). First, the shower cores should be located in the LHAASO-KM2A to get a good geometry reconstruction. So events with core located in a circle with radius from 180m to 500m and centered at the center of the array are chosen. Second, in order to get a full Cherenkov image, events with the arrival directions in a circle with the 4° radius and centered in the center of the FOV of the telescope are chosen, thirdly, the events with Rp less than 50m are discarded in order to avoid the saturation of the SiPM.

At the studied energy range the flux is very low, the effective area should be as large as possible. So the effective Rp range that can be used, are studied. On one hand the Rp could be reached as far as possible, to get a large effective area, however, on the other hand, the effective area is geometry dependent as the energies of cosmic rays increase if the Rp is chosen very far. So different Rp ranges are studied in figure 6 (left). All of the three group results can be fitted by a constant line. According to figure 6 (left), the smaller Rp range lead to the less geometrical dependent as the energies of cosmic ray increase. Considering the requirement of large effective area and less geometry dependent, Rp range with less than 250m can be used. With the above cuts, about $14000m^2Sr$ effective area can be obtained for all cosmic rays.

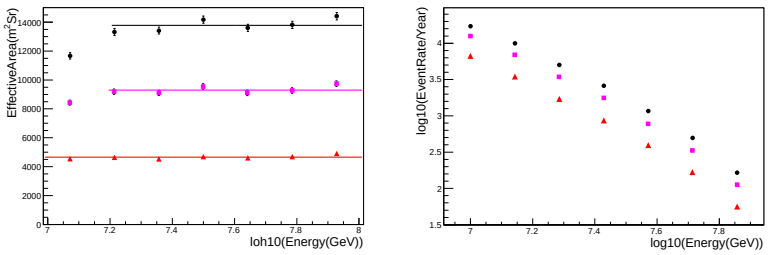

Figure 6: The effective area(left plot)and event rate (right plot) of LHAASO detectors. The black filled circles indicate the Rp range from 50m to 250m, the pink filled squres indicate the Rp range from 50m to 230m, and the red triangles indicate the Rp range from 50m 50 200m.

The integral event rate per year can be observed based on the Horandel model are also studied as shown in figure 6 (right). In the plot, 15% duty cycle are assumed, because LHAASO-WFCTA can only be worked in clear night without moon. At the high energy end 300 events are expected for year.

Besides the all cosmic rays effective area, the effective area of iron are also studied with more cuts the P_r with values less than -20 and $\delta\theta$ with values less than 0.8. The effective area and event rate of iron are shown in figure 7. According to figure 7, about $5000m^2Sr$ effective area can be obtained for iron detection. And about 100 events are expected based on the effective area according to Horandel model.

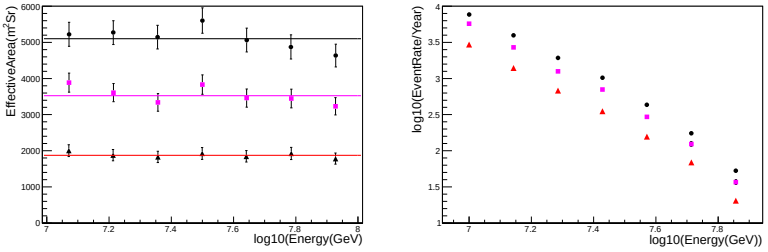

Figure 7: The effective area(left plot)and event rate (right plot) of LHAASO detectors for iron detection. The black filled circles indicate the Rp range from 50m to 250m, the pink filled squres indicate the Rp range from 50m to 230m, and the red triangles indicate the Rp range from 50m to 200m.

6. summary

The performance of hybrid observation of LHAASO-KM2A and LHAASO-WFCTA are studied in details. In primary elements identification, the P_r obtained from LHAASO-KM2A and $\delta\theta$ obtained from LHAASO-WFCTA can be used. The purity in selecting iron can reach 87%, while the the purity in selecting iron and MgAlSi can reach 94%. With some quality cuts, about $14,000m^2Sr$ effective area for all cosmic rays can be obtained with 15% duty cycle and 300 events are expected per year at the high energy end. After identification cuts, 100 iron events can be expected per year at the high energy end.

7. Acknowledgements

This work is supported by National Natural Science Foundation (NSFC) of China under contacts No. 11635011, 11505190, 11475190.

References

[1] J. R. Horandel, Astropart. Phys. 21, 241 (2004)

[2] J. Blumer, R. Engel, and J. R. Horandel, Prog. Part. Nucl. Phys. 63, 293 (2009).

[3] E. G. Berezhko, Astrophys. J. 661, L175 (2007).

[4] D. Heck, et. al., Report No. FZKA6019, Forschungszentrum, 1998.

[5] B. Bartoli et al, PHYSICAL REVIEW D 92, 092005 (2015)